Aquatic Toxicology 213 (2019) 105227

Contents lists available at ScienceDirect

Aquatic Toxicology

journal homepage: www.elsevier.com/locate/aqtox

Additives migrating from 3D-printed plastic induce developmental toxicity and neuro-behavioural alterations in early life zebrafish (*Danio rerio*)

Milanga Walpitagama[a], Megan Carve[a], Alon M. Douek[b], Charlene Trestrail[a], Yutao Bai[a], Jan Kaslin[b], Donald Wlodkowic[a,*]

[a] The Phenomics Laboratory, School of Science, RMIT University, Melbourne, VIC, 3083, Australia
[b] Australian Regenerative Medicine Institute, Monash University, Clayton, VIC, 3800, Australia

ARTICLE INFO

Keywords:
3D printing
Plastic
Toxicity
Apoptosis
Development
Behaviour
Zebrafish

ABSTRACT

The environmental impact of exposure to 3D-printed plastics as well as potential migration of toxic chemicals from 3D-printed plastics remains largely unexplored. In this work we applied leachates from plastics fabricated using a stereolithography (SLA) process to early developmental stages of zebrafish (*Danio rerio*) to investigate developmental toxicity and neurotoxicity. Migration of unpolymerized photoinitiator, 1-hydroxycyclohexyl phenyl ketone (1 − HCHPK) from a plastic solid phase to aqueous media at up to 200 mg/L in the first 24 h was detected using gas chromatography–mass spectrometry. Both plastic extracts (LC_{50} 22.25% v/v) and 1 − HCHPK (LC_{50} 60 mg/L) induced mortality and teratogenicity within 48 h of exposure. Developmental toxicity correlated with *in situ* generation of reactive oxygen species (ROS), an increase in lipid peroxidation and protein carbonylation markers and enhanced activity of superoxide dismutase (SOD) and glutathione-S-transferase (GST) in embryos exposed to concentrations as low as 20% v/v for plastic extracts and 16 mg/L for 1 − HCHPK. ROS-induced cellular damage led to induction of caspase-dependent apoptosis which could be pharmacologically inhibited with both antioxidant ascorbic acid and a pan-caspase inhibitor. Neuro-behavioral analysis showed that exposure to plastic leachates reduced spontaneous embryonic movement in 24–36 hpf embryos. Plastic extracts in concentrations above 20% v/v induced rapid retardation of locomotion, changes in photomotor response and habituation to photic stimuli with progressive paralysis in 120 hpf larvae. Significantly decreased acetylcholinesterase (AChE) activity with lack of any CNS-specific apoptotic phenotypes as well as lack of changes in motor neuron density, axonal growth, muscle segment integrity or presence of myoseptal defects were detected upon exposure to plastic extracts during embryogenesis. Considering implications of the results for environmental risk assessment and the growing usage of 3D-printing technologies, we speculate that some 3D-printed plastic waste may represent a significant and yet very poorly uncharacterized environmental hazard that merits further investigation on a range of aquatic and terrestrial species.

1. Introduction

Every year approximately three hundred million tonnes of plastics are manufactured worldwide and predominantly used in the packaging and construction industry (Hammer et al., 2012; Jambeck et al., 2015; PlasticsEurope, 2015). Due to global overuse of plastic products and their improper disposal, large amounts of plastic waste are deposited in aquatic ecosystems (Karbalaei et al., 2018). Plastic pollution can cause harm directly by ingestion and entanglement (Hammer et al., 2012; Karbalaei et al., 2018; Rochman et al., 2013; Wang et al., 2018). The long-term physiological impact of exposure to compounds that migrate from plastic to the immediate environment, such as bisphenol A (BPA), polybrominated diphenyl ethers (PBDE), phthalates and nonylphenols, still remains relatively unknown (Hermabessiere et al., 2017; Li et al., 2016; Lithner et al., 2011, 2012; OECD, 2004; Roh et al., 2013).

A recent study demonstrated that leachates from common recyclable plastics such as vinyl polymers (high-density polyethylene, HDPE; low-density polyethylene, LDPE; polypropylene, PP; polyvinyl chloride, PVC), polyesters (polycarbonate, PC; polyethylene terephthalate, PET) and aromatic polymers (polystyrene, PS) significantly impact survival and settlement of larval stages of the marine barnacle *Amphibalanus (Balanus) amphitrite* (Li et al., 2016). Hydrophobic organic molecules migrating from plasticized PVC, epoxy products and polyurethane were also found to induce acute toxicity in *Daphnia magna* while PET

* Corresponding author at: The Phenomics Laboratory, School of Science, RMIT University, Plenty Road, PO Box 71, Bundoora, VIC 3083, Australia.
E-mail address: donald.wlodkowic@rmit.edu.au (D. Wlodkowic).

https://doi.org/10.1016/j.aquatox.2019.105227
Received 7 March 2019; Received in revised form 11 June 2019; Accepted 13 June 2019
Available online 13 June 2019
0166-445X/

leaching from mineral water bottles exhibited endocrine-disrupting effects in mudsnails (Lithner et al., 2009, 2012; Wagner and Oehlmann, 2009, 2011). Furthermore, BPA leaching predominantly from waste materials such as food and beverage containers was detected at concentrations of up to 4 µg/L in samples of freshwater and wastewater (Huang et al., 2012).

While endocrine-disrupting properties of BPA and its alternatives with similar structure such as bisphenol S (BPS) have been widely demonstrated (Zhang et al., 2017), the developmental neurotoxicity of BPA and BPS has only recently been postulated (Chen et al., 2017; Gu et al., 2019; Kinch et al., 2015; Liu et al., 2018; Zhou et al., 2017). Other much less characterized plastic additives such as polymerization photoinitiators 1-hydroxycyclohexyl phenyl ketone (1 − HCHPK) and 2-methyl-4′-(methyl-thio)-2-morpholinopropiophenone (MTMP) have also been recently detected as leaching from polyethylene ampoules used for intravenous injections, intravenous injection bags as well as disposable plastic syringes and syringe filters (Lee et al., 2015; Takai et al., 2018; Yamaji et al., 2012). Exposure to 1 − HCHPK induced cytotoxicity in *in vitro* assays on human cells and frame-shift mutations in Ames assays (Kawasaki et al., 2015; Takai et al., 2018). Interestingly, biologically active chemicals leaching from plastic laboratory consumables was shown to exhibit neurotoxic properties such as inhibition of nicotinic acetylcholine receptors, *N*-methyl-D-aspartate (NMDA) receptors, and L-type calcium channels (Glossmann et al., 1993), interference with monoamine oxidase (McDonald et al., 2008), activation of G-protein-coupled fatty acid receptors (Watson et al., 2009), and disruption of neurite development in cultured hippocampal neurons (Lee et al., 2015). Since many low molecular weight plastic additives are used ubiquitously in the manufacturing of various plastic polymers and appear to exhibit phenotypes associated with toxicity, their migration to aqueous phases may represent an nascent ecotoxicological risk for both freshwater and marine organisms as well as human health (Hermabessiere et al., 2017).

Adding to the issues discussed above are new sources of plastic manufacturing, such as 3D printing. These often use spatially controlled photopolymerization of liquid photoreactive polymers to create plastic parts, and the end products are composed of different cross-linked polymer chains, photoinitiator residues, additives (*e.g.* stabilisers, antioxidants, lubricants, acid scavengers, anti-static agents, pigments, and fillers), and metabolites such as free-radicals (Carve and Wlodkowic, 2018; Ligon et al., 2017). The non-polymerized residues that reside in the 3D printed plastic are usually of low molecular weight and are either unbound or weakly bound to the polymeric macromolecular scaffold (Carve and Wlodkowic, 2018). Consequently, they can readily migrate from the plastics upon contact with aqueous media (Carve and Wlodkowic, 2018; Ferraz et al., 2018; Macdonald et al., 2016; Zhu et al., 2015b). Despite the mounting evidence of cytotoxic, endocrine disrupting and sub-lethal neurotoxic properties of plastic additives, the characterization of the environmental implications of 3D printed plastic has so far largely avoided scrutiny and in-depth investigations (Carve and Wlodkowic, 2018; Ferraz et al., 2018; Macdonald et al., 2016; Zhu et al., 2015b). The photoreactive polymer resins are composed of a diverse range of plastic monomers, oligomers, and complex additives that can be potentially harmful to both aquatic and terrestrial biota (Carve and Wlodkowic, 2018; Ferraz et al., 2018; Ligon et al., 2017; Zhu et al., 2015a). In addition, disposal of 3D printing by-products, such as out-of-date liquid polymer resins, and volumes of solvents contaminated with unpolymerized residues used in various post-processing steps, can be yet another source of potential environmental hazards (Carve and Wlodkowic, 2018; Zhu et al., 2015a).

In this work, we applied early developmental stages of zebrafish (*Danio rerio*) as proxy models to investigate potential adverse effects of leachates from 3D printed plastic on aquatic biota. In particular, considering recent reports on neurotoxic properties of chemicals derived from laboratory and clinical plastic consumables, our goals were to identify if any unpolymerized residues that migrate out of 3D-printed plastic can induce developmental toxicity and neurotoxicity during exposure in vertebrate early life stages. Importantly, we show that leachates from 3D-printed plastics induce oxidative stress, apoptosis and profound neuro-behavioural alterations. Our data signify possible environmental risks associated with 3D-printing of plastics that warrant further in-depth exploratory studies.

2. Materials and methods

2.1. Chemicals

Chemicals and solvents were procured from Sigma-Aldrich (Australia). Stock solutions of 1-hydroxycyclohexyl-phenylketone (1 − HCHPK, C16H13O2, molecular weight 204.26 g/mol, CAS No. 947-19-3) were prepared by dissolving the chemical in HPLC-grade dimethyl sulfoxide (DMSO) and stored in 25 mL amber glass bottles at 4 °C in darkness. Stability of the stock solution was monitored using gas chromatography-mass spectrometry (GC–MS; see below for details). E3 embryo medium (5 mM NaCl, 0.17 mM KCl, 0.33 mM CaCl2, 0.33 mM MgSO4, and 0.01% Methylene Blue as a fungicide) was used for dilution of 1 − HCHPK and plastic extract treatments, and for negative controls.

2.2. Stereolithography and aqueous extraction of plastics

A block shaped object with a surface area of 6,250 mm^2, and a volume of 3,263.71 mm^3 was 3D printed in Form Clear photoreactive resin (Formlabs Inc., Somerville, MA, USA) using the Form 1 SLA system (Formlabs Inc). Plastic parts were soaked in 100% isopropyl alcohol (IPA) for 10 min to remove any un-polymerised resin residues, followed by air-drying, and 12 h exposure to UV light (HWS-120, Clyde Apac). Leachates from 3D printed plastic parts were obtained by placing four of the 3D printed plastic blocks in a glass bottle filled with 1000 mL of embryo medium (15.66 g/L, solid-to-liquid ratio), for 24 h at 22 ± 1 °C with constant magnetic stirring at 240 rpm. Extractions were conducted in darkness to avoid photodegradation of leached compounds, such as light-sensitive photoinitiators.

2.3. Zebrafish husbandry

Wild type zebrafish (*Danio rerio*, Tübingen strain), double-transgenic *Tg(isl1:GFP)* (Higashijima et al., 2000)*, Tg(actc1b:mCherry-CAAX)* (Berger et al., 2014), and single transgenic *Tg(-.35ubb:secANXA5-mVenus)* (Morsch et al., 2015) lines, were kept in recirculating 3 L tanks on a 14:10 h light: dark cycle, and maintained according to standard protocol at 27 ± 0.5 °C, and pH at 7.0–7.5 at the Monash University AquaCore Facility. E3 embryo medium was used for zebrafish embryo culture. Use of animals was subject to standard Monash University Animal Welfare Committee regulations and protocols.

2.4. Developmental toxicity with embryos and eleuthero-embryos

Fish embryo toxicity assay (FET) was performed according to DIN 38415-6 (2001), with minor modifications. Briefly, embryos (5 hpf, Tübingen strain) were exposed to plastic extract (20, 30, 40, 60, 80, or 100% v/v), or 1 − HCHPK (20, 40, 60, 80, 100 mg/L), or control treatments. At 48 hpf, four lethal endpoints (coagulation of embryo, lack of somite formation, non-detachment of the tail, and lack of heartbeat) were scored. Assays were deemed valid if mortality in the negative control group (E3 embryo media) was < 10%, and mortality in the positive controls (4 mg/L of 3,4-dichloroaniline) was between 30 and 80%. Toxicity tests with eleuthero-embryos (120 hpf, Tübingen strain) were performed as described previously (Huang et al., 2018b). Eleuthero-embryos were exposed to plastic extract (20, 30, 40, 60, 80, or 100% v/v) or control (E3 embryo media) treatments. At 48 h following the commencement of treatment, presence or absence of lethal

endpoints (lack of touch response and heartbeat) was assessed. DMSO within all groups never exceeded 0.1%. All assays were conducted in darkness at 28 ± 0.5 °C. Experiments were conducted in duplicated with 20 embryos or eleuthero-embryos per treatment group.

2.5. Gas chromatography–mass spectrometry (GC–MS)

GC–MS analysis was performed using a Agilent 6890 N gas chromatograph/mass selective detector (GC/MSD) system (Agilent Technologies Australia Pty. Ltd., Forest Hill, Victoria, Australia). The plastic extract was concentrated by freeze-drying for 72 h, and then dissolved in dichloromethane at a ratio of 600:1 (w/v). Separation was performed on an Agilent DB-5 ms column (30 m × 0.25 mm, 0.25 µm). All injections were split (split ratio was 1:20) and the injection volume was 1 µL. The flow rate (He) was 0.8 mL min^{-1}. The injector temperature was set at 250 °C. The column temperature ramping was programmed from 40 °C (1 min) to 325 °C at 10 °C min^{-1} intervals. The final temperature step of 325 °C was maintained for 4.5 min. Data were acquired in the electron impact (EI) mode using selected ion monitoring (SIM). The obtained spectra were identified against the National Institute of Standards and Technology (NIST; USA) library. Percent confidence was reported for each peak assigned to a library match. For quantification of 1 − HCHPK in plastic extracts, calibration standards were prepared by serial diultion with HPLC-grade dimethyl DMSO (0–250 mg/L).

2.6. Measurement of oxidation-reduction potential (ORP)

Measurements of oxidation-reduction potential (ORP) of plastic extract (10 and 20%), 1 − HCHPK (16 and 60 mg/L), control (E3 embryo media), and positive control (H_2O_2) solutions were performed using 781 pH/Ion Meter (Metrohm Australia, Gladesville, Australia) equipped with a Pt ring/Ag-AgCl ORP electrode (Metrohm). Measurements of plastic extracts and 1 − HCHPK were performed at RT in both Milli-Q water and embryo medium. Hydrogen peroxide (H_2O_2) was used as a reference for high oxidative potential.

2.7. In situ detection of ROS

Untreated (Control, E3 embryo media) and treated (20% v/v extract, and 60 mg/L 1 − HCHPK) zebrafish embryos (48 hpf, Tübingen strain, n = 20) were immersed in 1 µM of dichloro-fluorescein-diacetate (H_2DCFDA) at 28 °C for 30 min, as previously described (Mugoni et al., 2014), and H_2DCFDA was removed by washing embryos briefly in fresh medium. Embryos anesthetized with 0.04% MS222 (Tricaine, Sigma) were mounted in low melting point agarose and imaged using a Nikon SMZ18 fluorescent stereomicroscope using bandpass filters for GFP/FITC (Ex: 488 nm, Em: 510 nm).

2.8. Biochemical analyses

2.8.1. Sample preparation

Normal zebrafish embryos (5 hpf, Tübingen strain) were exposed to plastic extract (10 or 20% v/v), 1 − HCHPK (16 or 60 mg/L), or control treatments, and incubated in darkness at 28 ± 0.5 °C. At 48 hpf, embryos were snap-frozen on dry ice in 500 µl phosphate buffered saline (pH 7) containing EDTA-free protease inhibitor cocktail (Sigmafast™, Sigma), and stored at −80 °C for subsequent assays. Immediately prior to analysis, samples were thawed on ice and cells were disrupted using a manual, micro tissue stick-homogeniser. Samples were centrifuged at 5000 x g for 10 min at 4 °C, and the supernatant was retained for analysis. Unless otherwise stated, all assays were conducted in triplicate at room temperature and measured in a plate reader (POLARstar Omega, BMG LABTECH GmbH). Results were normalised to protein content of the samples, which was measured with Bradford reagent (Sigma) using bovine serum albumin as standard. Hydrogen peroxide (H_2O_2, 10 mM) was the negative control for assays measuring lipid peroxidation (malondialdehyde, MDA) and protein carbonyl content. Lead (100 µg/L) was the negative control for assays measuring catalase, superoxide dismutase, and glutathione S-transferase activity.

2.8.2. Lipid peroxidation assay

Oxidative damage to lipids was determined by monitoring the reaction of MDA with thiobarbituric acid using the thiobarbituric acid reactive substance (TBARS) assay as described in (Parrilla-Taylor et al., 2013). TBARS content was calculated using the extinction coefficient of 155 mM^{-1} cm^{-1}, and results were expressed as nM TBARS mg $protein^{-1}$.

2.8.3. Protein carbonylation assay

Oxidative damage to intracellular proteins was determined by quantifying the content of protein carbonyls as described before (Mesquita et al., 2014), and using the extinction coefficient 22 308 M^{-1} cm^{-1}. Results were presented as nM mg protein $^{-1}$.

2.8.4. Glutathione-S-transferase (GST, EC 2.5.1.18) activity assay

GST activity was quantified by the method (Frasco and Guilhermino, 2002). GST activity was expressed as nM substrate hydrolysed min^{-1} mg $protein^{-1}$.

2.8.5. Superoxide dismutase (SOD, EC1.15.1.1) activity assay

Total SOD activity was measured using the method described by Vazquez-Medina et al (2012). Enzymatic activity was expressed in U mg $protein^{-1}$, with one unit defined as the amount of enzyme needed to inhibit the blank reaction rate by 50%.

2.8.6. Catalase (CAT, E.C. 1.11.1.6) activity assay

CAT activity was measured as in (Hadwan and Abed, 2016) and expressed as kU min^{-1} mg $protein^{-1}$.

2.8.7. Acetylcholinesterase (AChE, EC 3.1.1.7) activity assay

AChE activity was measured using the procedure of Ellman et al. (Ellman et al., 1961) adapted to a microplate reader as described in (Guilhermino et al., 1996). AChE activity was determined using the extinction coefficient 14050 M^{-1} cm^{-1}, and presented as nM substrate hydrolysed min^{-1} mg $protein^{-1}$.

2.9. Whole-mount immunohistochemistry (caspase 3 activation)

To assess activation of caspase-3 as a marker of caspase-dependent apoptosis, whole-mount immunofluorescence staining with anti-active caspase-3 monoclonal antibody (Abcam, ab2302, 1:1000 dilution) and an Alexa Fluor 555 secondary antibody (ThermoFisher, A-21429, 1:2000 dilution) was performed as described before (Sorrells et al., 2013). Staurosporine (200 µg/L), a pan-kinase inhibitor was used as a positive control. Untreated (Control, E3 embryo media) and treated (20% v/v extract, and 60 mg/L 1 − HCHPK) zebrafish embryos (48 hpf, Tübingen strain, n = 20) were mounted in 70% glycerol for fluorescence confocal imaging using a Leica TCS SP8 confocal microscope equipped with a HyD detector using filters for GFP (Ex: 488 nm, Em: 510 nm) and the Alexa 555 fluorophore (Ex: 555 nm, Em: 580 nm). Active caspase-3 positive cells across the whole embryo were manually counted with ImageJ software as described before (Skommer et al., 2006).

2.10. Externalisation of phosphatidylserine residues (Annexin A5 affinity) assay

In situ externalization of phosphatidylserine residues (a marker of early stages of apoptosis), was assessed using a transgenic line *Tg (-3.5ubb:secANXA5-mVenus)* which drives an mVenus-labelled secreted human Annexin 5 under the control of a 3.5 kb ubiquitin b promoter.

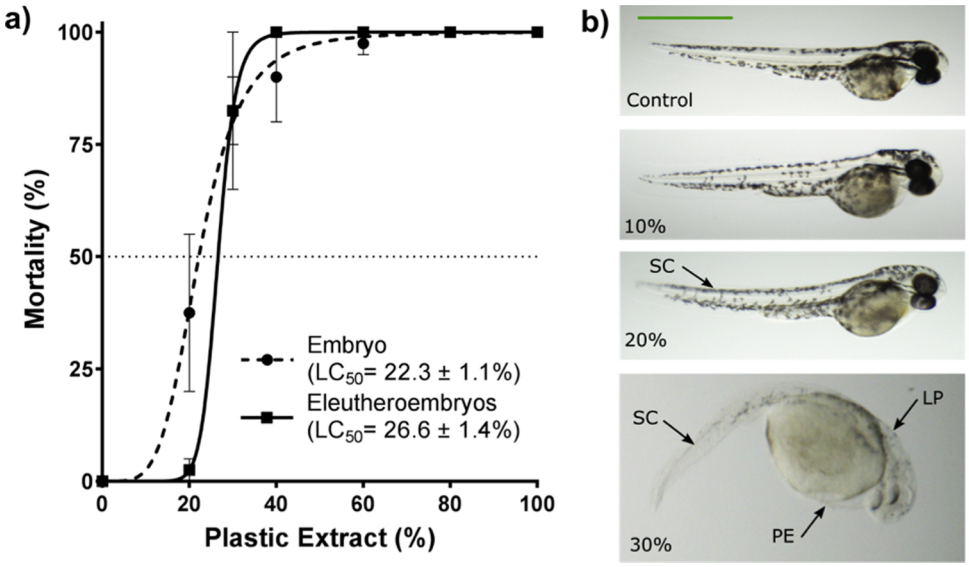

Fig. 1. Sublethal and lethal effects upon exposure of zebrafish (*Danio rerio*) to plastic extracts for up to 48 h: (a) dose-response curves for 5 hpf embryos and 120 hpf eleutheroembryos; (b) representative images of sub-lethal effects upon exposure to plastic extract in 48 hpf embryos (SC: spinal curvature, LP: lack of pigmentation, PE: pericardial edema). Data is mean ± S.E, n = 40 with least squares (ordinary) fit. Scale bar is 1 mm.

Briefly, 5 hpf embryos were exposed to the selected treatments up to 24 hpf, then anaesthetised in 0.04% tricaine methanesulfonate (MS-222) followed by fixation in 2% paraformaldehyde (PFA) in 0.1 M phosphate buffer. Embryos were mounted in 70% glycerol for fluorescence imaging performed with an Olympus MVX10 fluorescent stereomicroscope using bandpass filters for YFP (Ex: 497 nm, Em: 535 nm). The number of YFP-positive cells was manually counted with ImageJ software as described before (Skommer et al., 2006).

2.11. Primary motor neuron morphology and muscle development

Changes in motor neuron density, axonal growth, and presence of myoseptal defects were evaluated using a double-transgenic zebrafish line *Tg(isl1:GFP), Tg(actc1b:mCherry-CAAX)* – reporting for inter/motor neurons (GFP) and skeletal muscle (mCherry-CAAX) respectively. After exposure to selected treatments at 5 hpf, embryos were anesthetized in 0.04% tricaine methanesulfonate (MS-222) at 48 hpf followed by overnight fixation in 2% PFA in 0.1 M phosphate buffer at 4 °C. Fixed specimens were washed in 1x PBS and mounted in 70% glycerol for fluorescence confocal imaging. Imaging was performed with Leica TCS SP8 confocal microscope equipped with a HyD detector using filters for GFP (Ex: 488 nm, Em: 510 nm) and mCherry fluorophores (Ex: 587 nm, Em: 610 nm).

2.12. Embryo spontaneous activity (ESA) assay

Early developmental neurotoxicity was assessed using the Embryo Spontaneous Activity (ESA) behavioural assay, which quantifies spontaneous tail contractions in 24–36 hpf embryos, as described in (Raftery et al., 2014). Briefly, embryos (24 hpf, Tübingen strain) were exposed to plastic extract treatments (10, 20, 40, 50, 80, or 100% v/v, and control), and maintained in darkness at 27 ± 0.5 °C. At 25, 30 and 36 hpf behavioural responses were recorded under transmitted light using a custom video imaging system. Video files were analysed with DanioScope software (Noldus Inc, Wageningen, Netherlands), which quantified embryo burst movement, counts per minute and average duration.

2.13. Larval photomotor response (LPR) assay

The larval photomotor response (LPR) behavioural assay was performed using a ViewPoint Zebrabox system and video tracking software (ViewPoint Life Sciences, Lyon, France) as described before (Huang et al., 2018b). Eleuthero-embryos (120 hpf, Tübingen strain) were exposed to plastic extract treatments (20, 40, and 60% v/v) or control. Locomotor activity was assessed for a total of 60 min using alternating 4 h light and 4 h dark cycles. The larval dark startle response was obtained by subtracting the activity in dark periods from basal activity in the light periods. The area under the curve (AUC) was calculated to determine mean distance traveled, and light to dark acceleration was calculated using linear regression modeling of the last minute of the light cycle to the second minute of the dark cycle.

2.14. Data analysis

Statistical analysis, fitting of dose-response curves, and determination of LC_{50} values were performed with Prism 8 (GraphPad, San Diego, CA, USA) using inhibitor vs. normalized response least square fit, and a variable slope model. The normality of distribution was tested with the D'Agostino & Pearson normality test, and the homogeneity of variances was tested by the Brown-Forsythe test prior to ANOVA. Two-way ANOVA was used to test for treatment effects in toxicity evaluation, ESA tests, and active caspase and annexin V assays. One-way ANOVA was used to test for treatment effects in LPR and all other biochemical assays. When significant differences were found, Dunnett's or Sidak multiple comparisons tests were performed to identify significance between treatments and control. Statistical significance was defined as $p < 0.05$. Data are presented as means ± standard error (SE).

3. Results

3.1. Developmental toxicity of plastic extracts in zebrafish embryos

Initial dose response profiling tests showed significant onset of mortality in 5 hpf embryos (LC_{50} 22.25 ± 1.0%, n = 20). Eleuthero-embryos (120 hpf) exposed to plastic extracts for 48 h showed a similar survival rate (LC_{50} 26.62 ± 1.4%) (Fig. 1A). At 48 h post-treatment, eleuthero-embryos exposed to 20–100% extract exhibited three characteristic gross morphological developmental phenotypes: kinked spine/axis curvature, heart oedema, and decreased skin pigmentation (Fig. 1B). Exposure to lower levels of plastic extracts (up to 10%) did not induce any substantial onset of these developmental malformations.

3.2. Small molecule plastic additives migrate from plastics and induce developmental mortality

To determine possible toxic species in the plastic extracts, gas chromatography – mass spectrometry (GC – MS) analysis was

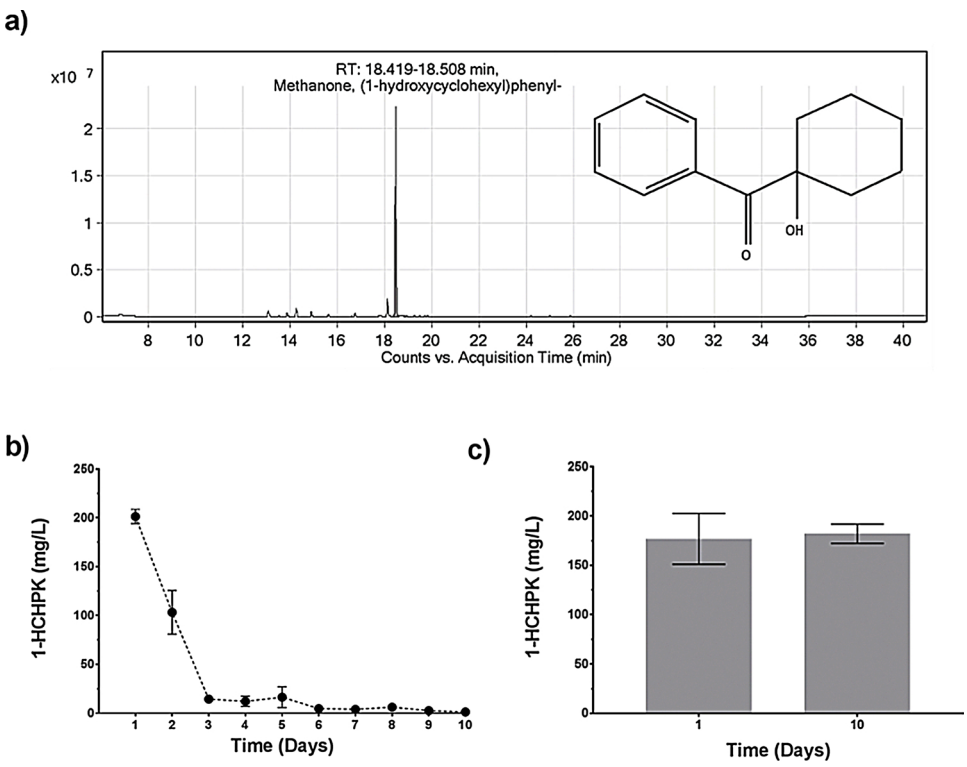

Fig. 2. Gas-Chromatography/Mass-Spectrometry analysis of plastics extracts: (a) chromatogram (counts *vs* acquisition time) depicting the presence of a compound identified as Methanone (1-hyrdroxycyclohexyl)phenyl, 1 − HCHPK, RT: 18.483 min, 97% match to the database entry) as well as a range of low concentrations of unidentified small molecular weight molecules, (b) leaching rate of 1 − HCHPK (mg/L) from a plastic in freshwater; (c) stability of the 1 − HCHPK (mg/L) when stored in darkness at room temperature. Data is presented as mean ± S.E (n = 3).

Table 1
Qualitative characterization of 3D-printed plastic extract using gas chromatography − mass spectrometry (GC − MS).

Compound	RT	Score	Purpose
Diphenyl sulfide	16.758	91.2	Initiator of or possible metabolite of an initiator such as 4-benzoyl-4'- methyl diphenyl sulfide
Dicumyl Peroxide	7.232	90.57	Thermal initiator
Benzoic acid, 2,4,6- trimethyl-,trimethylsilyl ester	14.903	89.99	Additive stabilizer
Methanone, (1-hydroxycyclohexyl)phenyl-	18.483	87.77	photopolymerization initiator
2-Ethy1-2- phenylaziridine	18.123	82.6	
mesityl-acetone	18.428	82.18	
3-Methylene-1-oxaspi ro[4.5] decan-2-one	13.879	81.74	Additive to minimise shrinkage

performed on the leachate. GC–MS identified the presence of the photoinitiator compound 1-hydroxycyclohexyl phenyl ketone (1 − HCHPK; Methanone) as a main constituent (RT: 18.483, score: 87.77) (Fig. 2A, Table 1). Six other compounds were detected with an identification score above 80, albeit at low levels as depicted by the GC–MS chromatogram (Fig. 2A, Table 1). These compounds were benzoic acid (RT: 14.903, score: 89.99), 3-Methylene-1-oxaspiro[4.5]decan-2-one (RT: 13.879, score: 81.74), dicumyl peroxide (RT: 7.232, score: 90.57), diphenyl sulphide (RT: 16.758, score: 91.2), 2-Ethyl-2-phenylaziridine (RT: 18.123, score: 82.6), and mesityl-acetone (RT: 18.428, score: 82.18) (Table 1).

Subsequently, time-resolved quantitative GC–MS analysis revealed that 1 − HCHPK migrated rapidly from the plastic solid phase with concentrations of 170–200 mg/L achieved after first 24 h of extraction in an aqueous medium (Fig. 2B). The leaching of 1 − HCHPK continued for up to 72 h with a total concentration achieved of aproximately 330–350 mg/L (Fig. 2B). At the same time the leaching rate of 1 − HCHPK at 48 h was half that at 24 h while the plastic solid phase was completely depleted of the unbound photoinitiator after 72 h of extraction in embryo medium (Fig. 2B). When stored in darkness, 1 − HCHPK was stable in aquatic medium with no significant changes in concentration (Fig. 2C).

To determine if 1 − HCHPK was a contributor to plastic extract toxicity, a FET test was conducted. Exposure of 1 − HCPK was lethal to embryos with LC_{50} of 60 mg/L and with concentrations above 20 mg/L inducing > 80% developmental malformations in surviving embryos such as spine curvature, heart oedema and an overt decrease in skin pigmentation.

3.3. Plastic leachates induce oxidative stress in developing embryos

To estimate the redox status of the plastic extract, the oxidation-reduction potential (ORP) was assessed. Plastic extracts and 1 − HCHPK were characterized by a very high oxidative potential (> 350 mV) (Fig. 3A).

The H_2DCFDA fluorescence assay indicated that zebrafish exposed to plastic extract (20%) or 1 − HCHPK (60 mg/L) had increased *in situ* ROS generation than controls (Fig. 3B). Biochemical markers of oxidative damage, lipid peroxidation (TBARS) and protein carbonylation were also elevated. Specimens exposed to 20% plastic extract or 60 mg/L 1 − HCHPK (Fig. 3C and D) had higher levels of protein oxidation than control. Specimens exposed to 60 mg/L 1 − HCHPK had higher levels of lipid peroxidation than control.

The activity of CAT was significantly lower in embryos exposed to 20% plastic extract as well as 16 and 60 mg/L 1 − HCHPK relative to negative controls (Fig. 4A; $p < 0.05$). In contrast, the activity of SOD was significantly elevated in all exposure scenarios relative to negative controls (Fig. 4B; $p < 0.05$). Similarly, GST activity indicated an overall trend of higher activity, albeit this was significant only in embryos exposed to 60 mg/L 1 − HCHPK (Fig. 4C; $p < 0.05$).

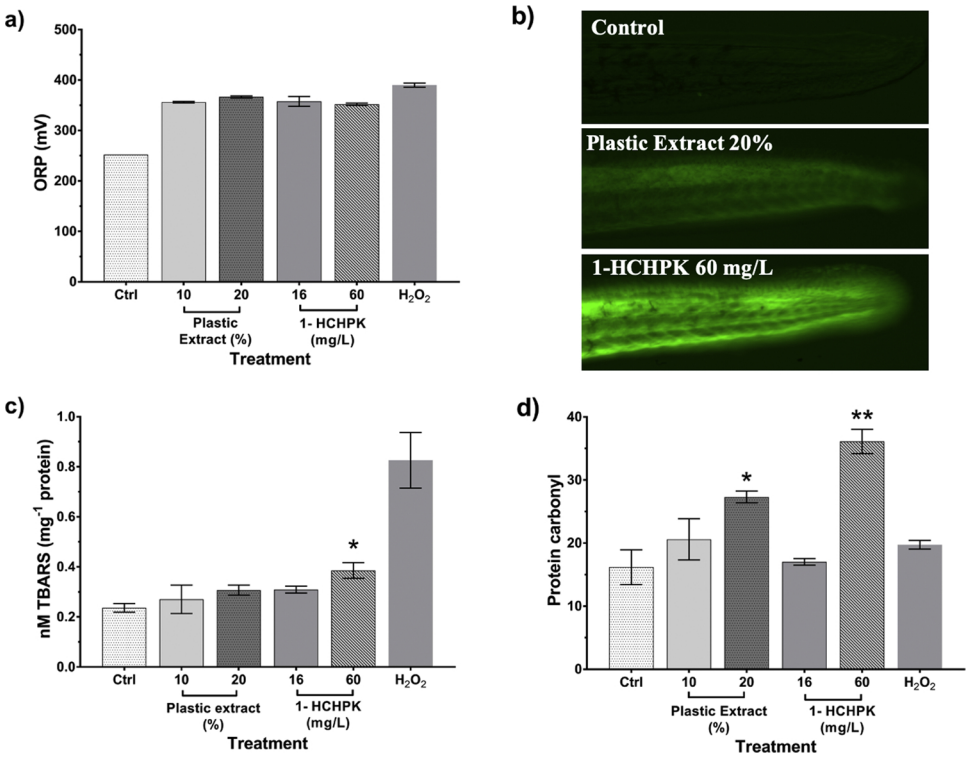

Fig. 3. Oxidative stress response in *Danio rerio* embryos exposed at 5 hpf to plastic extract (10 and 20% v/v), 1 − HCHPK (16 and 60 mg/L), or control treatments. (a) Estimation of the oxidation-reduction potential (ORP); (b) *In situ* imaging of ROS generation using dichlorofluorescein-diacetate (H_2DCFDA) in 48 hpf zebrafish embryos; (c) lipid peroxidation (MDA content) and (d) protein carbonylation upon exposure to selected treatments for 48 h. Hydrogen peroxide (H_2O_2) was used as a positive control (+Ctrl), and E3 embryo media was used as the negative control (- Ctrl). Results are shown as mean ± S.E, n = 3. Significant difference between treatment and control indicated by asterisks (One-way ANOVA, Dunnett's test, * $p < 0.05$, ** $p < 0.01$).

3.4. ROS-induced developmental toxicity is associated with elevated levels of apoptosis

To determine if the ROS-induced developmental toxicity was associated with elevated levels of apoptosis, a transgenic zebrafish reporter line for apoptotic cells, *Tg(-3.5ubb:secANXA5-mVenus),* was used to quantitate dying cells in embryos exposed to toxicants (Fig. 5A). Exposure to both plastic extract (20%) and 1 − HCHPK (60 mg/L) from 5 to 24 hpf significantly elevated the number of mVenus$^+$ cells in developing embryos relative to controls (Fig. 5A and B). The apoptotic phenotype in plastic extract (20%) and 1 − HCHPK (60 mg/L) treated embryos could be partially rescued by co-treatment with a ROS scavenger, ascorbic acid (80 mg/L), which significantly reduced the number of apoptotic mVenus$^+$ cells ($p < 0.01$, n = 20, Fig. 5B). Pharmacological rescue experiments with a well-established synthetic and irreversible pan-caspase inhibitor (z-VAD-fmk) showed significant reduction in the number of apoptotic cells, defined by immunostaining with an antibody against apoptotic marker cleaved caspase 3 in embryos treated with plastic extract (20%), 1 − HCHPK (60 mg/L) in combination with z-VAD-fmk (300 µM) ($p < 0.05$, n = 20, Fig. 5C).

Taken together, the data suggest that 3D printed plastic leachates induce toxicity and subsequent developmental abnormalities in zebrafish embryos via oxidative damage and subsequent downstream activation of caspase-dependent apoptotic cell death.

3.5. Plastic leachates inhibit spontaneous activity in early zebrafish embryos

To determine the impact of leachates on neural development, changes to the stereotypic embryonic locomotion patterns were determined. Zebrafish embryos display sensory-independent, spontaneous side-to-side tail contractions from 19 hpf onwards; changes to this twitching movement can be used as an early marker of neurotoxicity (Raftery et al., 2014). Exposure to 80% and 100% plastic extract at 24 hpf stage significantly affected this behaviour even after 1 h of exposure, when burst count/minute (defined as the number of tail contractions per minute) was lower for treated embryos (n = 20, $p < 0.05$) relative to control groups (Fig. 6A). The duration of twitches was also lower for treated embryos compared to controls (Fig. 6A; n = 20, $p < 0.05$). After 12 h of exposure to plastic extracts (36 hpf), burst count per minute was lower for embryos treated with 60, 80, and 100% leachate than control (Fig. 6A; n = 20, $p < 0.05$). Burst duration (defined as the length of tail contractions) was lower for embryos in the 60, 80, and 100% treatment groups than control (Fig. 6A; n = 20, $p < 0.05$). The duration of inactivity was also reduced in the 20% treatment group, and longer in embryos treated with the 40%, 80%, and 100% leachates (n = 20, $p < 0.05$) compared to controls (not shown).

3.6. Motor neuron and axial muscle development is unaffected by the toxicants

To assess whether the observed neurobehavioural changes were related to abnormalities in primary motor neuron morphology, axon outgrowth, muscle segment integrity or the presence of myoseptal defects during embryogenesis, *in situ* fluorescent imaging using the double-transgenic zebrafish fluorescent reporter line *Tg(isl1:GFP), Tg (actc1b:mCherry-CAAX)*, which reports for motor neurons and ventral interneurons, and skeletal muscle respectively, was used (Fig. 6B). It was observed that in surviving embryos, despite the onset of characteristic morphological abnormalities induced by toxicant exposure, neither plastic extracts nor 1 − HCHPK affected neurite outgrowth or the morphology or distribution of spinal motor neurons or interneurons (Fig. 6B). Furthermore, no gross changes in muscle segment integrity or myoseptal organisation were detected in treated embryos (Fig. 6B). This data suggests that the behavioural defects observed in embryonic locomotion after treatment with leachate were not associated with obvious neuro-muscular developmental abnormalities.

3.7. Embryo hypoactivity correlates with a decreased activity of acetylcholinesterase (AChE)

To determine if locomotor hypoactivity was caused by altered neuromuscular neurotransmission, the level of acetylcholinesterase was assessed after toxin exposure. Acetylcholine is a key neurotransmitter at

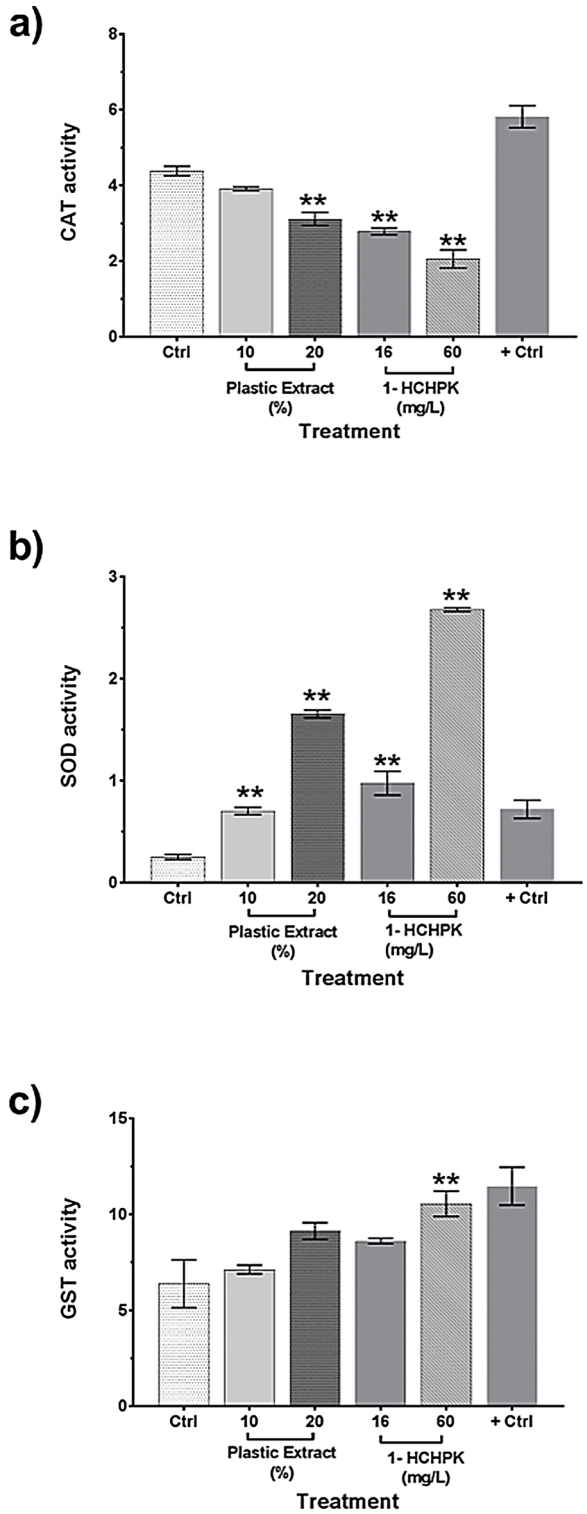

Fig. 4. Activity of oxidative defence enzymes in *Danio rerio* exposed to 10 or 20% plastic extract, or 16 or 60 mg/L 1 − HCHPK for up to 48 h: (a) Catalase (CAT) activity, (b) Superoxide dismutase (SOD) activity, and (c) Glutathione S-Transferase (GST) activity. Results are shown as mean ± S.E, n = 3. Significant difference between treatment and control indicated by asterisks (one-way ANOVA, Dunnett's test, * $p < 0.05$, ** $p < 0.01$).

the neuromuscular junction, and AChE is a key enzyme in the degradation of acetylcholine at neuromuscular synapses. In 48 hpf embryos, AChE activity was significantly lower in embryos exposed to plastic extract (10 or 20% v/v, $p < 0.05$) or 1 − HCHPK (15 or 60 mg/L, $p < 0.05$), than controls (Fig. 6C). Most notably, the reduction of AChE activity upon exposure to 20% v/v of plastic extract and 60 mg/L 1 − HCHPK (44.25% and 43.12%, respectively, $p < 0.05$) was strikingly similar to that achieved by a treatment with Chlorpyrifos a organophosphate pesticide (OP) which acts as a specific inhibitor of AChE and was used as as positive control (Fig. 6C).

3.8. Plastic additives alter the photomotor responses in larval zebrafish

To explore neurobehavioural endpoints upon toxicant exposure, we investigated the locomotor effects of exposure to plastic leachate and 1 − HCHPK under alternating light-dark photoperiod stimulation. Representative locomotor trajectories of 120 hpf larvae are presented in Fig. 7A. The total distance traveled was significantly lower in treatment groups relative to control groups in all concentrations tested, with 20% and 40% v/v extracts inducing approximately 25% and 50% locomotor retardation after 60 min of exposure ($p < 0.05$), respectively (Fig. 7B). Treatments with 20, 40, 60, 80 and 100% v/v of plastic extracts reduced the average swimming velocity by 30.2, 34.0, 18.5, 59.5 and 63.3 cm/min ($p < 0.05$), respectively. The average acceleration was also significantly reduced in concentrations above 40% v/v ($p < 0.05$; Fig. 7C). Further, in line with the neurobehavioural assays conducted at earlier developmental time points, a slight increase in acceleration was observed in larvae treated with 20% v/v plastic extract compared to untreated controls.

The analysis of light-dark cycle photomotor responses revealed significant reductions in photokinesis at all tested concentrations, with an overall decrease in locomotor activity in response to both dark and light stimuli (Fig. 7D and E). Treatment with all tested concentrations invoked significant and progressive hypoactivity in dark-startle response (Fig. 7D and E). A decrease in distance moved, following treatment with 20% v/v extract, was prevalent during first two photoperiod cycles, whereas effects of higher concentrations were ubiquitous in all dark-startle cycles (Fig. 7E). Similar effects were also observed upon exposure of larvae to 1 − HCHPK, with the manifestation of a statistically significant hypoactivity phenotype observed above 30 mg/L ($p < 0.05$, Supplementary Fig. 1).

Taken together, the chemobehavioural phenotyping provides evidence that small molecular weight chemicals migrating from 3D printed plastics can profoundly alter behavior. The rapid onset of neurobehavioral changes suggests pleiotropic activity with a different mechanism of action to that identified for developmental toxicity.

4. Discussion

4.1. 3D printed plastic additives as emerging micropollutants

Despite mounting evidence of cytotoxic, endocrine disrupting and sub-lethal neurotoxic properties of plastic additives, the environmental risks associated with exposure to 3D printed plastics and the by-products of 3D printing (such as contaminated solvents used in post-processing of plastic parts as well as out-of-date photoreactive resins) have so far largely avoided scrutiny. SLA-based 3D printing of plastics in particular uses controlled photopolymerization of liquid photoreactive polymer resins. As demonstrated in this work, the migration of plastic additives, such as the photoinitiator 1 − HCHPK, can rapidly occur upon contact of plastic with water. These non-polymerized residues are typically present in excess, and are usually of low molecular weight and either weakly bound, or not bound at all to the plastic macromolecular scaffold (Carve and Wlodkowic, 2018; Yamaji et al., 2012).

To date, a handful of reports have indicated the toxicity of 3D printed plastic parts and/or the low molecular weight additives migrating out of them (Ferraz et al., 2018; Macdonald et al., 2016; Oskui et al., 2016; Zhu et al., 2015a). These reports have not been widely recognised in the environmental science community because they were primarily aimed at evaluation of plastic biocompatibility for specific

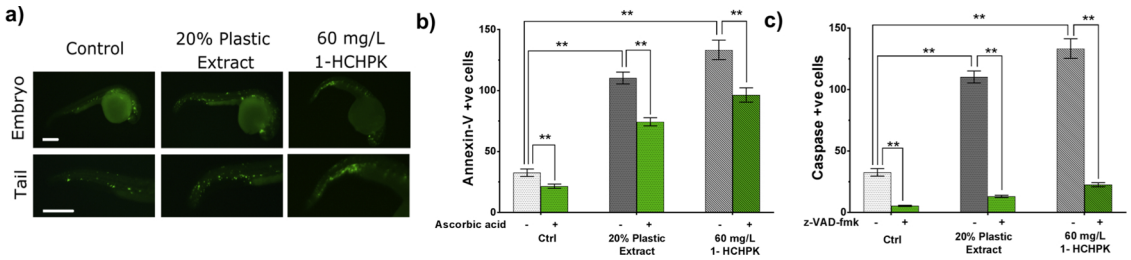

Fig. 5. Impact of plastic additives on induction of caspase-dependent apoptosis in zebrafish embryos exposed to toxicants for up to 48 h. (a) representative fluorescence imaging of transgenic *Tg(-3.5ubb:secANXA5-mVenus)* embryos; (b) quantification of annexin-positive cells in transgenic *Tg(-3.5ubb:secANXA5-mVenus)* embryos upon co-treatment with (+) or without (-) an antioxidant ascorbic acid; (c) quantification of cleaved caspase 3-positive cells in wild type embryos upon co-treatment with (+) or without (-) a synthetic pan-caspase inhibitor (z-VAD-fmk, 300 µM). Data is mean ± S.E (n = 10), scale bar = 250 µm. Significant difference between treatment and control indicated by asterisks (Two-way ANOVA, Tukey's test, * $p < 0.05$, ** $p < 0.01$).

applications in bioengineering and fabrication of biomedical devices (Carve and Wlodkowic, 2018; Zhu et al., 2015a). These studies align with the findings of our current work and collectively indicate that unregulated 3D printed plastic waste can potentially exert harmful effects on the environment. Furthermore, as new manufacturing technologies mature and flourish, one can expect dramatically increasing volumes of 3D printed waste reaching the environment. We postulate that greater systematic review of chemical risks associated with 3D printed plastic pollutants is highly warranted before larger streams of waste find their way into the aquasphere.

4.2. Developmental toxicity of 3D plastic additives

The potential of 3D-printed materials to induce developmental toxicity is an important consideration due to the increasing domestic and commercial uses of these products, and the possible ecological consequences of exposure during vertebrate embryonic development being largely unknown (Carve and Wlodkowic, 2018). In this study, we demonstrated that both crude leachates from 3D printed parts as well as the identified main constituent, photoinitiator 1−HCHPK, induce significant developmental toxicity in embryonic zebrafish. Previous studies have detected 1−HCHPK in intravenous injection solutions, and in food products after it had migrated from plastic products or printing ink used in labelling (Jung et al., 2013; Yamaji et al., 2012). Subsequent toxicity profiling determined that 1−HCHPK is cytotoxic in human fetal osteoblasts, bovine chondrocytes, and human monocytes (Kawasaki et al., 2015; Williams et al., 2005; Yamaji et al., 2012) (Kawasaki et al. 2015, Yamaji et al., 2012; Williams et al., 2005), and it has endocrine disrupting effects (Morizane et al., 2015).

We speculate that the mechanism of toxicity is directly linked to oxidative damage in developing embryos. The corroborating evidence was provided by a high oxidative potential of both crude leachate and the photoinitiator as well as *in situ* detection of ROS generation, elevated markers of oxidative stress and enzymes involved in oxidative defense mechanisms. Further, we hypothesize that developmental toxicity of plastic additives can be linked to primary and/or secondary mitochondrial dysfunction that in turn leads to a catastrophic increase in ROS and subsequent initiation of apoptosis. Any chemical that can induce a significant redox imbalance can induce dysfunction in organelles such as mitochondria and the endomembrane system, which act as sentinels of intracellular damage (Jaattela, 2002; Skommer et al., 2007). In our work we did not directly investigate the impact of toxicants on the mitochondrial function and bioenergetics or the stability of the endomembrane system. However, a recent study by Liang et al. (2019) demonstrated that benzotriazole ultraviolet stabilizers found in many commercial plastics induce oxidative stress and alter the mitochondrial bioenergetics. Similarly, a recent study demonstrated that exposure to a plastic precursor, bisphenol S (BPS), in early stages of development significantly enhanced oxidative stress in zebrafish (Gu et al., 2019).

In line with the above studies, our data showing increased activity of SOD coupled with elevated markers of oxidative damage suggest that the antioxidant defense systems were activated in our treated samples due to redox imbalance (Cai et al., 2012; Gu et al., 2019; Liang et al., 2019). Given the significant increase in the SOD activity, it is plausible that significantly high concentrations of H_2O_2, decreased evidence of CAT activity. Previous work has demonstrated substrate inhibition in presence of excess H_2O_2 reduces CAT activity (Altomare et al., 1974; Maharajan et al., 2018; Vasudevan and Weiland, 1990). Taken together, this data indicates that compounds migrating from 3D printed plastics can induce dose-dependent oxidative stress.

Alterations in homeostasis of the mitochondrial network and endoplasmic reticulum is commonly associated with a further secondary increase in levels of ROS (*e.g.* due to mitochondrial uncoupling and dissipation of inner mitochondrial membrane potential) and, in most instances, irreparable damage that activates one of the programmed cell death pathways such as caspase-dependent apoptosis (Jaattela, 2002; Skommer et al., 2007). In line with this, we provided evidence that the molecular foundations of developmental toxicity associated with 3D-printed plastic leachates link oxidative stress to downstream activation of caspase-depended cell death. The pharmacological rescue of chemically-induced phenotypes using antioxidants and the pan-caspase inhibitor, z-VAD-fmk, support the hypotheses of of ROS-induced apoptosis, and that this is most likely one of the main mechanisms of toxicity induced by plastic additives. This highlights the caspase-dependent apoptosis pathway as critical and causative for developmental mortality in our experimental context. Several studies have also provided evidence of systemic toxicity induced by plastic additive compounds (Ruszkiewicz et al., 2017), and induced apoptosis in both zebrafish and murine macrophages has been demonstrated (Gu et al., 2019; Huang et al., 2018a).

4.3. Neurobehavioural alterations induced by 3D-printed plastic additives

A growing number of studies indicate neurotoxic effects of small molecular weight plastic additives that leach into aquatic media in both *in vitro* and diverse animal models (Chen et al., 2017; Gu et al., 2019; Lee et al., 2015; Liang et al., 2019; Liu et al., 2018; Zhou et al., 2017). However, the developmental neurotoxicity and impact of 3D printed plastic additives on the developing CNS remains largely unknown.

It has been previously demonstrated that chemobehavioral phenotyping in early stages of zebrafish can be applied as sensitive endpoints for detecting neurotoxicity induced by environmental toxicants (Raftery et al., 2014). In this work, we identified the photoinitiator 1−HCHPK as a major constituent of the 3D-printed plastic leachate, and demonstrate that exposure to plastic leachates and 1−HCHPK alone reduced spontaneous embryonic movement in 24–36 hpf embryos. Crude plastic extracts in concentrations above 20% v/v as well as 1−HCHPK above 30 mg/L also induced rapid retardation of locomotion, changes in photomotor response and habituation to photic stimuli

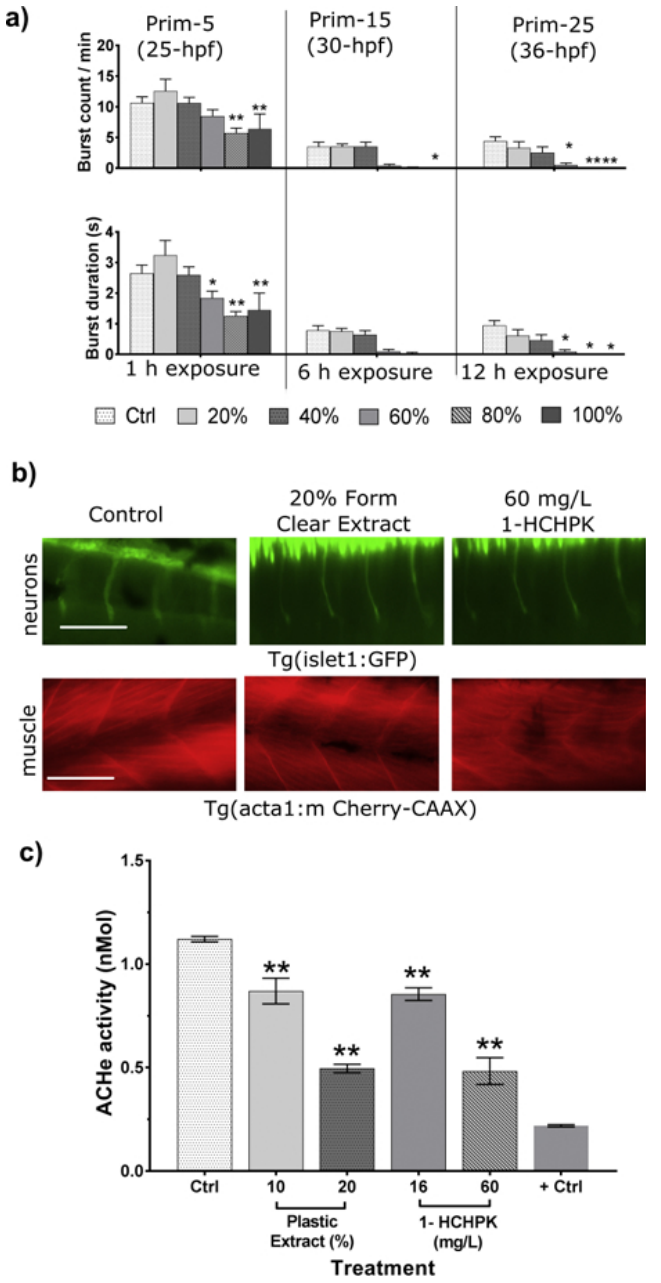

Fig. 6. Impact of plastic additives on neuro-behavioural endpoints in early developmental stages of zebrafish. (a) quantification of spontaneous tail contractions (upper panel - burst count per minute; lower panel - burst duration) upon exposure to selected treatments for 1, 6, and 12 h; (b) fluorescence imaging using a double transgenic *Tg(isl1:GFP), Tg(actc1b:mCherry-CAAX)* line showing development of motor/ventral interneurons (upper panel) and skeletal muscle (lower panel); (c) activity of acetylcholinesterase (AChE) in embryos exposed to plastic additives. Organophosphate Chlorpyrifos was used as a positive control. Results are shown as mean ± S.E, n = 3. Significant difference between treatment and positive control indicated by asterisks (ANOVA, Dunnett's test, * $p < 0.05$, ** $p < 0.01$).

with progressive paralysis in 120 hpf larvae when exposed for up to 60 min. Hypoactivity in both embryonic and larval stages following short-term exposures suggest that plastic additives migrating from the solid phase induces rapid, functional neurophysiological effects. Furthermore, the significant disturbance of photokinesis in the light/dark-startle assays performed indicates abnormalities associated with neuronal pathways involved in behavioral responses to light. These conclusions are further supported by decreased levels of acetylcholinesterase (AChE) activity upon exposure to those toxicants with lack of any CNS-specific apoptotic phenotypes as well as lack of gross changes in inter/motor neuron density, axonal growth, muscle segment integrity or presence of myoseptal defects. Interestingly, several recent studies demonstrated similar neuro-behavioural alterations upon exposure to other plastic additives such as benzotriazole ultraviolet stabilizers, BPA and BPS as well as BPA-induced inhibition of cholinergic signaling regarded as a classical biomarker of neurotoxicity (Chen et al., 2017; Gu et al., 2019; Liang et al., 2019).

Considering our earlier findings of ROS-induced developmental toxicity, we cannot discard another plausible hypothesis that may imply systemic rather than specifically neurological foundations of the behavioural phenotypes observed in this study. Namely, we anticipate that significant mitochondrial toxicity leading to rapid uncoupling of the electron transport chain and a subsequent reduction in oxidative phosphorylation and thus ATP levels will likely manifest itself in a gross hypoactive phenotype. Considering that treatment of zebrafish embryos in larvae in all assays in this study were performed by immersion, we acknowledge it is plausible that systemic effects on the level of mitochondrial bioenergetics or proportionate overexposure of toxicants to the peripheral nervous system could induce anesthetic symptoms without any specific primary target in the CNS.

It should be noted that plastic additives might exhibit a specifically neural mode of action. Several studies have reported that plastic additives disrupt neurite development in cultured hippocampal neurons, inhibit nicotinic acetylcholine, NMDA receptors, and L-type calcium channels (Gu et al., 2019; Lee et al., 2015; Liu et al., 2018). The results of or study, which found a significant decrease in AChE activity, a canonical marker of neurotoxicity, taken together with other reports, are in suport of the specifically neural mode of action hypothesis.

Chemobehavioral phenotyping is reported to be highly sensitive at detecting neuroactive chemicals; however, we recognize that even if effects of toxicants are neurospecific, the hypoactivity during early development may not result in any long-term locomotive defects nor may it manifest as sensorimotor and/or cognitive deficits at later stages of development. We nevertheless postulate that the collective body of evidence indicating impacts of plastic additives on neuro-behavioural phenotypes requires further investigation with diverse models to elucidate if they have neurological and/or systemic bioenergetic foundations.

5. Conclusions

Data presented in this work supplement a growing number of reports on the acute toxicity of plastics leachates for aquatic biota. Surprisingly, there is a paucity of data regarding the chemical composition and toxicological effects of plastics manufactured using rapidly growing additive manufacturing technologies that are collectively referred to as three-dimensional printing.

In this work we demonstrate that small molecular weight additives can rapidly migrate from the solid phase of 3D printed plastics into aqueous media. The additives identified are predominantly photopolymerization initiators and stabilizers, which can induce significant developmental toxicity and neuro-behavioural perturbations upon exposure in early stages of vertebrate development. To the best of our knowledge, this is also the first report to show a causative link between oxidative stress and caspase-dependent apoptosis upon exposure to 3D-printed plastic additives during vertebrate development.

We postulate that emerging plastic manufacturing technologies such as 3D printing can potentially increase the risks associated with chemical exposure to complex mixtures of new and poorly characterized micro-pollutants in both aquatic and terrestrial ecosystems. Further research into the effects of plastic additives after longer-term exposure is required to provide a broader validation for the neurotoxicity endpoints observed here. Additional cellular and molecular phenotypes, such as mitochondrial toxicity, should also be explored as they may

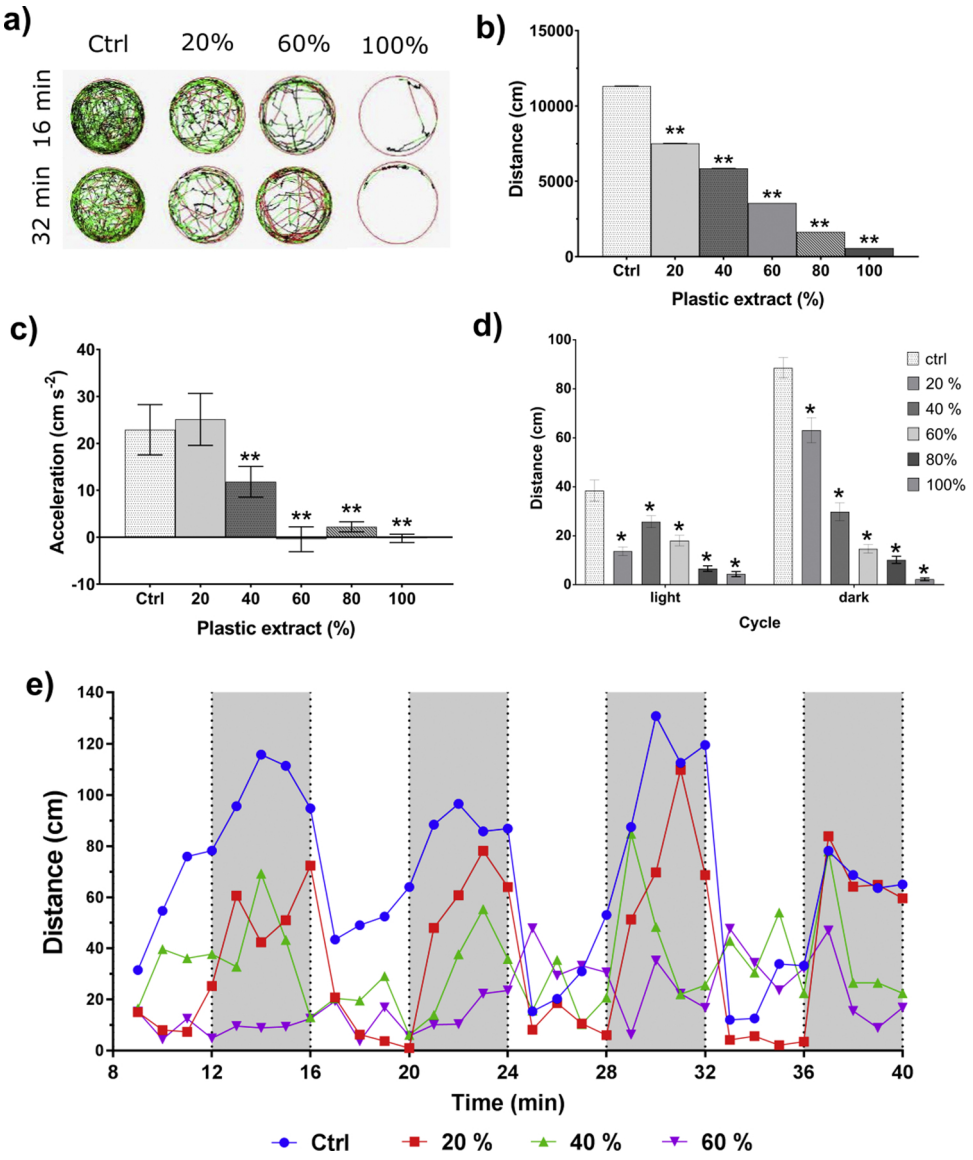

Fig. 7. Effects of additives leaching from 3D printed plastics on photomotor behavioural responses in 120 hpf zebrafish larvae. (a) reconstruction of representative locomotion trajectories; (b) quantification of changes in a total distance travelled and (c) acceleration over 60 min of exposure; (d) quantification of changes in total distance traveled in dark vs. light cycles; (e) time-resolved analysis of light-dark cycle photomotor behaviors. Data is mean ± S.E (n = 30). Significant differences between treatment and controls indicated by asterisks (* $p < 0.05$, ** $p < 0.01$, One-way ANOVA, Dunnett's test).

underpin the rapid behavioral perturbations observed in this study. Collectively the data outlined in this work signify possible environmental risks associated with 3D-printing of plastics, which warrant further in-depth exploratory studies.

Acknowledgments

This project was funded by Australian Research Council Grant No DE130101046 (DW); RMIT Vice-Chancellor's Senior Research Fellowship (DW); NHMRC project grants GNT1068411, GNT1145048 and GNT 1138870 (JK); Monash University Faculty of Medicine and Nursing strategic grant (JK); Operational Infrastructure Support from the Victorian Government (JK). The Australian Regenerative Medicine Institute is supported by grants from the State Government of Victoria and the Australian Government.

Authors thank Monash Micro Imaging (MMI) facility, Monash University, for technical imaging support as well as staff of the FishCore, Monash University, for microscope access and support with zebrafish husbandry.

Authors declare no competing financial interests.

Appendix A. Supplementary data

Supplementary material related to this article can be found, in the online version, at doi:https://doi.org/10.1016/j.aquatox.2019.105227.

References

Altomare, R.E., Kohler, J., Greenfield, P.F., Kittrell, J.R., 1974. Deactivation of immobilized beef liver catalase by hydrogen peroxide. Biotechnol. Bioeng. 16, 1659–1673.

Berger, J., Tarakci, H., Berger, S., Li, M., Hall, T.E., Arner, A., Currie, P.D., 2014. Loss of Tropomodulin4 in the zebrafish mutant trage causes cytoplasmic rod formation and muscle weakness reminiscent of nemaline myopathy. Dis. Model. Mech. 7, 1407–1415.

Cai, G., Zhu, J., Shen, C., Cui, Y., Du, J., Chen, X., 2012. The effects of cobalt on the development, oxidative stress, and apoptosis in zebrafish embryos. Biol. Trace Elem. Res. 150, 200–207.

Carve, M., Wlodkowic, D., 2018. 3D-printed chips: compatibility of additive manufacturing photopolymeric substrata with biological applications. MicromachinesBasel 9.

Chen, Q., Yin, D., Jia, Y., Schiwy, S., Legradi, J., Yang, S., Hollert, H., 2017. Enhanced uptake of BPA in the presence of nanoplastics can lead to neurotoxic effects in adult zebrafish. Sci. Total Environ. 609, 1312–1321.
Ellman, G.L., Courtney, K.D., Andres, V., Featherstone, R.M., 1961. A new and rapid colorimetric determination of acetylcholinesterase activity. Biochem. Pharmacol. 7 88-&.
Ferraz, M.D.M.M., Henning, H.H.W., Costa, P.F., Malda, J., Le Gac, S., Bray, F., van Duursen, M.B.M., Brouwers, J.F., van de Lest, C.H.A., Bertijn, I., Kraneburg, L., Vos, P.L.A.M., Stout, T.A.E., Gadella, B.M., 2018. Potential health and environmental risks of three-dimensional engineered polymers. Environ Sci Tech Let 5, 80–85.
Frasco, M.F., Guilhermino, L., 2002. Effects of dimethoate and beta-naphthoflavone on selected biomarkers of Poecilia reticulata. Fish Physiol. Biochem. 26, 149–156.
Glossmann, H., Hering, S., Savchenko, A., Berger, W., Friedrich, K., Garcia, M.L., Goetz, M.A., Liesch, J.M., Zink, D.L., Kaczorowski, G.J., 1993. A light stabilizer (Tinuvin-770) that elutes from polypropylene plastic tubes is a potent L-Type Ca2+-Channel blocker. P Natl Acad Sci USA 90, 9523–9527.
Gu, J., Zhang, J., Chen, Y., Wang, H., Guo, M., Wang, L., Wang, Z., Wu, S., Shi, L., Gu, A., Ji, G., 2019. Neurobehavioral effects of bisphenol S exposure in early life stages of zebrafish larvae (Danio rerio). Chemosphere 217, 629–635.
Guilhermino, L., Lopes, M.C., Carvalho, A.P., Soares, A.M.V.M., 1996. Acetylcholinesterase activity in juveniles of Daphnia magna Straus. B Environ Contam Tox 57, 979–985.
Hadwan, M.H., Abed, H.N., 2016. Data supporting the spectrophotometric method for the estimation of catalase activity. Data Brief 6, 194–199.
Hammer, J., Kraak, M.H., Parsons, J.R., 2012. Plastics in the marine environment: the dark side of a modern gift. Rev. Environ. Contam. Toxicol. 220, 1–44.
Hermabessiere, L., Dehaut, A., Paul-Pont, I., Lacroix, C., Jezequel, R., Soudant, P., Duflos, G., 2017. Occurrence and effects of plastic additives on marine environments and organisms: a review. Chemosphere 182, 781–793.
Higashijima, S., Hotta, Y., Okamoto, H., 2000. Visualization of cranial motor neurons in live transgenic zebrafish expressing green fluorescent protein under the control of the islet-1 promoter/enhancer. J. Neurosci. 20, 206–218.
Huang, F.M., Chang, Y.C., Lee, S.S., Ho, Y.C., Yang, M.L., Lin, H.W., Kuan, Y.H., 2018a. Bisphenol A exhibits cytotoxic or genotoxic potential via oxidative stress-associated mitochondrial apoptotic pathway in murine macrophages. Food Chem. Toxicol. 122, 215–224.
Huang, Y.Q., Wong, C.K., Zheng, J.S., Bouwman, H., Barra, R., Wahlstrom, B., Neretin, L., Wong, M.H., 2012. Bisphenol A (BPA) in China: a review of sources, environmental levels, and potential human health impacts. Environ. Int. 42, 91–99.
Huang, Y.S., Cartlidge, R., Walpitagama, M., Kaslin, J., Campana, O., Wlodkowic, D., 2018b. Unsuitable use of DMSO for assessing behavioral endpoints in aquatic model species. Sci. Total Environ. 615, 107–114.
Jaattela, M., 2002. Programmed cell death: many ways for cells to die decently. Ann. Med. 34, 480–488.
Jambeck, J.R., Geyer, R., Wilcox, C., Siegler, T.R., Perryman, M., Andrady, A., Narayan, R., Law, K.L., 2015. Plastic waste inputs from land into the ocean. Science 347, 768–771.
Jung, T., Simat, T.J., Altkofer, W., Fugel, D., 2013. Survey on the occurrence of photo-initiators and amine synergists in cartonboard packaging on the German market and their migration into the packaged foodstuffs. Food Addit. Contam. Part A Chem. Anal. Control Expo. Risk Assess. 30, 1993–2016.
Karbalaei, S., Hanachi, P., Walker, T.R., Cole, M., 2018. Occurrence, sources, human health impacts and mitigation of microplastic pollution. Environ. Sci. Pollut. Res. Int. 25, 36046–36063.
Kawasaki, Y., Tsuboi, C., Yagi, K., Morizane, M., Masaoka, Y., Esumi, S., Kitamura, Y., Sendo, T., 2015. Photoinitiators enhanced 1,2-dichloropropane-induced cytotoxicity in human normal embryonic lung fibroblasts cells in vitro. Environ. Sci. Pollut. Res. Int. 22, 4763–4770.
Kinch, C.D., Ibhazehiebo, K., Jeong, J.H., Habibi, H.R., Kurrasch, D.M., 2015. Low-dose exposure to bisphenol A and replacement bisphenol S induces precocious hypothalamic neurogenesis in embryonic zebrafish. Proc Natl Acad Sci U S A 112, 1475–1480.
Lee, T.W., Tumanov, S., Villas-Boas, S.G., Montgomery, J.M., Birch, N.P., 2015. Chemicals eluting from disposable plastic syringes and syringe filters alter neurite growth, axogenesis and the microtubule cytoskeleton in cultured hippocampal neurons. J. Neurochem. 133, 53–65.
Li, H.X., Getzinger, G.J., Ferguson, P.L., Orihuela, B., Zhu, M., Rittschof, D., 2016. Effects of toxic leachate from commercial plastics on larval survival and settlement of the barnacle amphibalanus amphitrite. Environ. Sci. Technol. 50, 924–931.
Liang, X., Adamovsky, O., Souders 2nd, C.L., Martyniuk, C.J., 2019. Biological effects of the benzotriazole ultraviolet stabilizers UV-234 and UV-320 in early-staged zebrafish (Danio rerio). Environ Pollut 245, 272–281.
Ligon, S.C., Liska, R., Stampfl, J., Gurr, M., Mulhaupt, R., 2017. Polymers for 3D printing and customized additive manufacturing. Chem. Rev. 117, 10212–10290.
Lithner, D., Damberg, J., Dave, G., Larsson, K., 2009. Leachates from plastic consumer products–screening for toxicity with Daphnia magna. Chemosphere 74, 1195–1200.
Lithner, D., Larsson, A., Dave, G., 2011. Environmental and health hazard ranking and assessment of plastic polymers based on chemical composition. Sci. Total Environ. 409, 3309–3324.
Lithner, D., Nordensvan, I., Dave, G., 2012. Comparative acute toxicity of leachates from plastic products made of polypropylene, polyethylene, PVC, acrylonitrile-butadiene-styrene, and epoxy to Daphnia magna. Environ. Sci. Pollut. Res. Int. 19, 1763–1772.
Liu, W., Zhang, X., Wei, P., Tian, H., Wang, W., Ru, S., 2018. Long-term exposure to bisphenol S damages the visual system and reduces the tracking capability of male zebrafish (Danio rerio). J. Appl. Toxicol. 38, 248–258.
Macdonald, N.P., Zhu, F., Hall, C.J., Reboud, J., Crosier, P.S., Patton, E.E., Wlodkowic, D., Cooper, J.M., 2016. Assessment of biocompatibility of 3D printed photopolymers using zebrafish embryo toxicity assays. Lab Chip 16, 291–297.
Maharajan, K., Muthulakshmi, S., Nataraj, B., Ramesh, M., Kadirvelu, K., 2018. Toxicity assessment of pyriproxyfen in vertebrate model zebrafish embryos (Danio rerio): a multi biomarker study. Aquat. Toxicol. 196, 132–145.
McDonald, G.R., Hudson, A.L., Dunn, S.M.J., You, H.T., Baker, G.B., Whittal, R.M., Martin, J.W., Jha, A., Edmondson, D.E., Holt, A., 2008. Bioactive contaminants Leach from disposable laboratory plasticware. Science 322 917-917.
Mesquita, C.S., Oliveira, R., Bento, F., Geraldo, D., Rodrigues, J.V., Marcos, J.C., 2014. Simplified 2,4-dinitrophenylhydrazine spectrophotometric assay for quantification of carbonyls in oxidized proteins. Anal. Biochem. 458, 69–71.
Morizane, M., Kawasaki, Y., Miura, T., Yagi, K., Esumi, S., Kitamura, Y., Sendo, T., 2015. Photoinitiator-initiated estrogenic activity in human breast Cancer cell line MCF-7. J Toxicol Environ Health A 78, 1450–1460.
Morsch, M., Radford, R., Lee, A., Don, E.K., Badrock, A.P., Hall, T.E., Cole, N.J., Chung, R., 2015. In vivo characterization of microglial engulfment of dying neurons in the zebrafish spinal cord. Front. Cell. Neurosci. 9, 321.
Mugoni, V., Camporeale, A., Santoro, M.M., 2014. Analysis of oxidative stress in zebrafish embryos. J. Vis. Exp.
OECD, O.E.Ha.S.P.E. Directorate, 2004. Emission Scenario Document on Plastic Additives. Paris.
Oskui, S.M., Diamante, G., Liao, C.Y., Shi, W., Gan, J., Schlenk, D., Grover, W.H., 2016. Assessing and reducing the toxicity of 3D-Printed parts. Environ Sci Tech Let 3, 1–6.
Parrilla-Taylor, D.P., Zenteno-Savin, T., Magallon-Barajas, F.J., 2013. Antioxidant enzyme activity in pacific whiteleg shrimp (Litopenaeus vannamei) in response to infection with white spot syndrome virus. Aquaculture 380, 41–46.
PlasticsEurope, 2015. Plastics the Facts. pp. 2014–2015.
Raftery, T.D., Isales, G.M., Yozzo, K.L., Volz, D.C., 2014. High-content screening assay for identification of chemicals impacting spontaneous activity in zebrafish embryos. Environ. Sci. Technol. 48, 804–810.
Rochman, C.M., Hoh, E., Hentschel, B.T., Kaye, S., 2013. Long-term field measurement of sorption of organic contaminants to five types of plastic pellets: implications for plastic marine debris. Environ. Sci. Technol. 47, 1646–1654.
Roh, J.Y., Kim, M.H., Kim, W.I., Kang, Y.Y., Shin, S.K., Kim, J.G., Kwon, J.H., 2013. Ecological risk assessment of chemicals migrated from a recycled plastic product. Environ. Health Toxicol. 28, e2013013.
Ruszkiewicz, J.A., Pinkas, A., Ferrer, B., Peres, T.V., Tsatsakis, A., Aschner, M., 2017. Neurotoxic effect of active ingredients in sunscreen products, a contemporary review. Toxicol. Rep. 4, 245–259.
Skommer, J., Wlodkowic, D., Deptala, A., 2007. Larger than life: mitochondria and the Bcl-2 family. Leuk. Res. 31, 277–286.
Skommer, J., Wlodkowic, D., Pelkonen, J., 2006. Cellular foundation of curcumin-induced apoptosis in follicular lymphoma cell lines. Exp. Hematol. 34, 463–474.
Sorrells, S., Toruno, C., Stewart, R.A., Jette, C., 2013. Analysis of apoptosis in zebrafish embryos by whole-mount immunofluorescence to detect activated Caspase 3. J. Vis. Exp., e51060.
Takai, M., Kawasaki, Y., Arimoto, S., Tanimoto, Y., Kitamura, Y., Sendo, T., 2018. UV-irradiated 2-methyl-4′-(methylthio)-2-morpholinopropiophenone-containing injection solution produced frameshift mutations in the Ames mutagenicity assay. Environ. Sci. Pollut. Res. Int. 25, 10135–10140.
Vasudevan, P.T., Weiland, R.H., 1990. Deactivation of catalase by hydrogen peroxide. Biotechnol. Bioeng. 36, 783–789.
Wagner, M., Oehlmann, J., 2009. Endocrine disruptors in bottled mineral water: total estrogenic burden and migration from plastic bottles. Environ. Sci. Pollut. Res. Int. 16, 278–286.
Wagner, M., Oehlmann, J., 2011. Endocrine disruptors in bottled mineral water: estrogenic activity in the E-Screen. J. Steroid Biochem. Mol. Biol. 127, 128–135.
Wang, F., Wong, C.S., Chen, D., Lu, X., Wang, F., Zeng, E.Y., 2018. Interaction of toxic chemicals with microplastics: a critical review. Water Res. 139, 208–219.
Watson, J., Greenough, E.B., Leet, J.E., Ford, M.J., Drexler, D.M., Belcastro, J.V., Herbst, J.J., Chatterjee, M., Banks, M., 2009. Extraction, identification, and functional characterization of a bioactive substance from automated compound-handling plastic tips. J. Biomol. Screen. 14, 566–572.
Williams, C.G., Malik, A.N., Kim, T.K., Manson, P.N., Elisseeff, J.H., 2005. Variable cytocompatibility of six cell lines with photoinitiators used for polymerizing hydrogels and cell encapsulation. Biomaterials 26, 1211–1218.
Yamaji, K., Kawasaki, Y., Yoshitome, K., Matsunaga, H., Sendo, T., 2012. Quantitation and human monocyte cytotoxicity of the polymerization agent 1-hydroxycyclohexyl phenyl ketone (Irgacure 184) from three brands of aqueous injection solution. Biol. Pharm. Bull. 35, 1821–1825.
Zhang, D.H., Zhou, E.X., Yang, Z.L., 2017. Waterborne exposure to BPS causes thyroid endocrine disruption in zebrafish larvae. PLoS One 12, e0176927.
Zhou, Y., Wang, Z., Xia, M., Zhuang, S., Gong, X., Pan, J., Li, C., Fan, R., Pang, Q., Lu, S., 2017. Neurotoxicity of low bisphenol A (BPA) exposure for young male mice: implications for children exposed to environmental levels of BPA. Environ Pollut 229, 40–48.
Zhu, F., Friedrich, T., Nugegoda, D., Kaslin, J., Wlodkowic, D., 2015a. Assessment of the biocompatibility of three-dimensional-printed polymers using multispecies toxicity tests. Biomicrofluidics 9.
Zhu, F., Skommer, J., Friedrich, T., Kaslin, J., Wlodkowic, D., 2015b. 3D printed polymers toxicity profiling - a caution for biodevice applications. Micro+Nano Materials, Devices, and Systems 9668.